Quantitative analysis of Argonaute protein reveals microRNA-dependent localization to stress granules

Anthony K. L. Leung*, J. Mauro Calabrese*, and Phillip A. Sharp*†‡

*Center for Cancer Research and †Department of Biology, Massachusetts Institute of Technology, Cambridge, MA 02139

Contributed by Phillip A. Sharp, October 6, 2006 (sent for review October 4, 2006)

Argonaute proteins associate with microRNAs (miRNAs) that bind mRNAs through partial base-pairings to primarily repress translation in animals. A fraction of Argonaute proteins and miRNAs biochemically cosediment with polyribosomes, yet another fraction paradoxically accumulates in ribosome-free processing bodies (PBs) in the cytoplasm. In this report, we give a quantitative account of the Argonaute protein localization and dynamics in living cells in different cellular states. We find that the majority of Argonaute is distributed diffusely in the cytoplasm, and, when cells are subjected to stress, Argonaute proteins accumulate to newly assembled structures known as stress granules (SGs) in addition to PBs. Argonaute proteins displayed distinct kinetics at different structures: exchange faster at SGs and much slower at PBs. Further, miRNAs are required for the Argonaute protein localization to SGs but not PBs. These quantitative kinetic data provide insights into miRNA-mediated repression.

fluorescence microscopy | processing bodies | post-transcriptional control | dynamics

MicroRNAs (miRNAs) are involved in diverse cellular and developmental roles in plants and animals (1, 2). They are predicted to regulate at least 30% of mammalian protein encoding mRNAs by interacting with their 3′ UTRs (3). Misregulation of miRNA expression can result in developmental defects and cancers (1, 4). In animals, most miRNAs repress translation, but the mechanism remains unclear (5, 6). Sucrose gradient fractionation revealed that both Argonaute protein, the signature component of the miRNA-associated ribonucleoparticle (miRNP) protein complex, and miRNAs consistently cosediment with polyribosomes (7–10). Further, miRNA-repressed target mRNAs are found to be substantially associated with polyribosome (8–11) and, to some degree, the monosome fraction (12), reflecting that miRNAs may regulate at translation either after initiation or at initiation, respectively.

In the cytoplasm, there are two cellular structures known to interact dynamically with mRNAs, namely processing bodies (PBs) and stress granules (SGs) (13). PBs are well characterized translation-incompetent sites for mRNA decay in the yeast *Saccharomyces cerevisiae* and mammalian cells. These structures contain enzymes responsible for decapping, deadenylation, and degradation but lack any ribosomal proteins. Interestingly, it has been suggested that nontranslating mRNAs localized at PBs, instead of being degraded, can reenter polyribosomes in yeast (14) and, perhaps, also in mammalian cells (15). Recently, PBs also were found to be associated with Argonaute proteins, mature miRNAs, and miRNA-repressed mRNAs (12, 15–20), raising the possibility that PBs might be involved in miRNA-mediated repression. Yet, subsequent data have shown that miRNA-mediated repression is unaffected in cells devoid of microscopically visible PBs (20), suggesting that PB formation itself is not required for the repression and such association may represent secondary events.

SGs are known to be sites where nontranslating, 40S ribosome-associated poly(A)+ mRNAs accumulate when cells experience stresses, such as heat shock, or osmotic or oxidative stress, or when translation initiation is specifically inhibited (13). Whether miRNAs or Argonaute proteins associate with this structure remains unknown. PBs and SGs are known to be dynamically associated with, and often juxtaposing, each other (21), and they share components, such as the cap-binding protein eIF4E and the translational repressor rck/p54; however, not all PB components are found in SGs, or vice versa (13). In this report, we quantitatively analyze the kinetics of Argonaute protein localization in mammalian cells, providing evidence that Argonaute proteins can localize to SGs and such association depends on the presence of miRNAs.

Results

Ago2 Localizes to the Diffuse Cytoplasm, PBs, and SGs. To quantitatively assess the extent of localization of Argonaute protein to PBs, we fused enhanced GFP to the amino terminus of human Argonaute protein 2 (EGFP-Ago2) and established HeLa cell lines stably expressing the fusion protein (Fig. 1*a*). Immunofluorescence analysis of these HeLa(EGFP-Ago2) cells demonstrated that the fusion protein colocalized with the endogenous Argonaute protein in PBs (arrows in Fig. 1*c*). Quantitative three-dimensional measurements revealed that ≈0.3% of the cytoplasmic volume constituted PBs and that the integrated intensities of EGFP-Ago2 at PBs accounted for ≈1.3% of the total fluorescence in the cytoplasm (Fig. 5, which is published as supporting information on the PNAS web site). These results are consistent with previous reports (12, 15–20) but show that the majority of the Argonaute protein is diffuse throughout the cytoplasm.

Previous studies have shown that miRNA-repressed mRNAs rapidly dissociate from polyribosomes upon inhibition of translation initiation by using an eIF4A-specific inhibitor hippuristanol (11). We next investigated where Argonaute protein localized under such conditions. Interestingly, upon addition of 1 μM hippuristanol for 30 min, EGFP-Ago2 accumulated at extra cytoplasmic foci (arrowheads in Fig. 1 *b* and *d*), which are not labeled by PB marker protein Dcp1a. These foci instead colocalized with the cytoplasmic pool of TIA1 (21), a nucleocytoplasmic shuttling protein that accumulates in SGs (Fig. 1*e*). Quantitatively, there was an ≈3-fold increase in the localization of EGFP-Ago2 at PBs and SGs in total after hippuristanol treatment (Fig. 5), suggesting that additional Argonaute proteins were redistributed from the diffuse cytoplasm to these distinct structures. Immunostaining with three different antibodies against Ago2 revealed the same colocalization pattern in SGs in parental HeLa cells, suggesting that the fusion protein faithfully reflects the localization of its endogenous counterpart (Fig. 1*f* and data not shown). Flag-tagged or GFP-tagged fusion proteins of all Argonaute protein family members (Ago1–4) also showed

Author contributions: A.K.L.L. and P.A.S. designed research; A.K.L.L. performed research; A.K.L.L. and J.M.C. contributed new reagents/analytic tools; A.K.L.L. and P.A.S. analyzed data; and A.K.L.L. and P.A.S. wrote the paper.

The authors declare no conflict of interest.

Abbreviations: miRNA, microRNA; PBs, processing bodies; SGs, stress granules; miRNP, miRNA-associated ribonucleoparticle; EGFP, enhanced GFP; TAMRA, tetramethylrhodamine.

‡To whom correspondence should be addressed. E-mail: sharppa@mit.edu.

CELL BIOLOGY

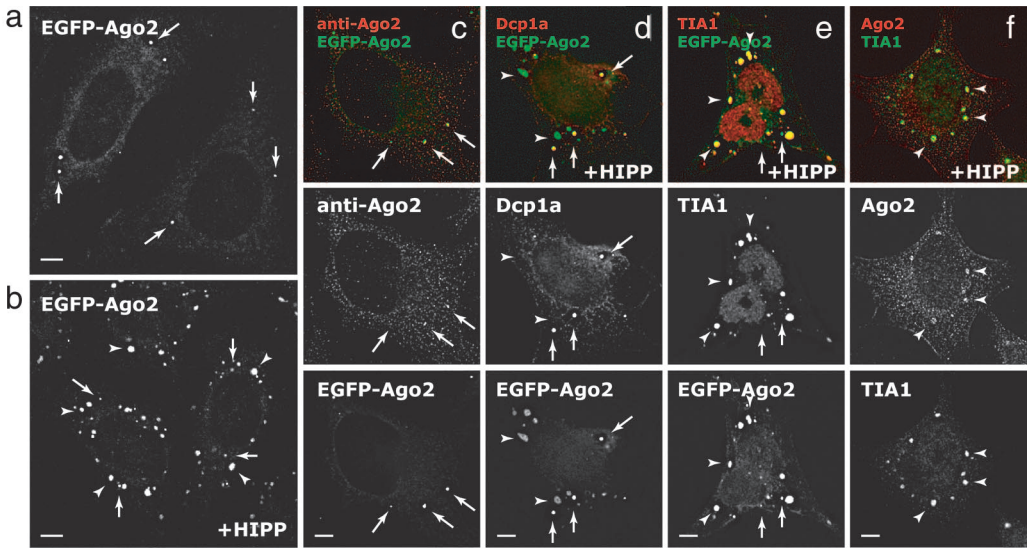

Fig. 1. Ago2 localizes to the cytoplasm, PBs, and SGs upon inhibition of translation initiation. (*a* and *b*) Stably expressed EGFP-Ago2 localized to the cytoplasm and PBs (arrows) (*a*) and, upon addition of 1 μM hippuristanol (HIPP) for 30 min, also localized to SGs (arrowheads) (*b*). (*c*) The localization of EGFP-Ago2 is the same as the endogenous Ago2 in the cytoplasm and PBs. (*d–f*) Upon addition of 1 μM HIPP, EGFP-Ago2 colocalized with PB marker Dcp1a (*d*) and SG marker TIA1 (*e*), and the endogenous Ago2 also colocalized with SG marker TIA1 in parental HeLa cells (*f*). (Scale bars, 5 μm.)

the same localization pattern when translation initiation was inhibited either in the presence of hippuristanol or under oxidative stress with arsenite (e.g., Fig. 2*e* and data not shown). Notably, under these conditions, luciferase reporter mRNAs containing three imperfectly complementary binding sites for endogenous miRNA *let-7a* (12), similar to EGFP-Ago2, also localized to PBs and SGs (Fig. 6, which is published as supporting information on the PNAS web site).

To assess whether the Argonaute protein at SGs originates from PBs or the cytoplasm, we followed the change in localization pattern in live HeLa(EGFP-Ago2) cells upon addition of hippuristanol. As early as 5–6 min after hippuristanol treatment,

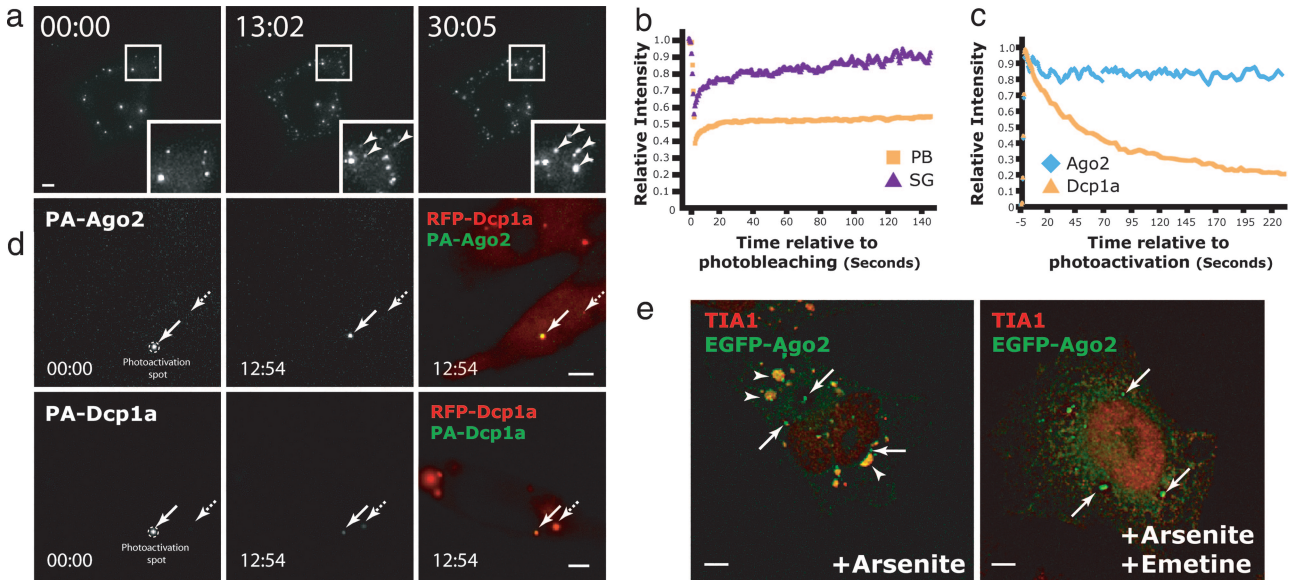

Fig. 2. Quantitative dynamics of Ago2 at PBs and SGs. (*a*) Time-lapse micrographs of stably expressed EGFP-Ago2 in a single live cell (complete movie is available in Movie 1). The first appearance of EGFP-Ago2 at SGs (arrowheads) occurred between 5 and 6 min after addition of 1 μM hippuristanol (HIPP). (*b*) Fluorescence recovery after photobleaching (FRAP) analyses of EGFP-Ago2 at single PBs (orange; $n = 5$) and SGs (purple; $n = 3$) and the intensities at respective structures relative to their initial intensities were compared over time. (*c* and *d*) PAGFP-Dcp1a and PAGFP-Ago2 were photoactivated at single PB labeled by mRFP-Dcp1a for 1 s, and the photoactivated cells were imaged over the next 13 min. (*c*) The intensities of PAGFP-Dcp1a (orange; $n = 3$) and PAGFP-Ago2 (blue; $n = 3$) at the photoactivated PBs were compared over time with their respective initial intensities after photoactivation. (*d*) Representative images of PAGFP-Ago2 (*Upper*) and PAGFP-Dcp1a (*Lower*) at $t = 00{:}00$ and 12:54. The intensity of PAGFP-Dcp1a decreased over time at the photoactivated PBs (arrows), whereas the one of PAGFP-Ago2 remained relatively constant over time. Also, it was observed that the intensities of PAGFP-Dcp1a gradually increased over time at the neighboring PBs (broken arrows; see also Fig. 7*e*), suggesting continuous exchange of Dcp1a between PBs and the cytoplasm. (*e*) Addition of emetine reduced the accumulation of EGFP-Ago2 at SGs labeled by TIA1 (red) even in the presence of continual oxidative stress (250 μM arsenite for 90 min). In this experiment, 10 μg/ml emetine (*Right*) or DMSO (*Left*) were added 30 min after the arsenite treatment and left for 60 min further before fixing the cell for immunolabeling with SG marker TIA1 and PB marker Dcp1a (data not shown). (Scale bars, 5 μm.)

EGFP-Ago2 accumulated at foci distinct from PBs in the cytoplasm (Fig. 2*a*; Fig. 7*a* and Movie 1, which are published as supporting information on the PNAS web site) and, notably, on a similar time scale when hippuristanol causes the dissociation of miRNA-repressed mRNAs from polyribosomes (11). These foci increased with time in number and size by multiple fusion events and were identified as SGs by TIA1 staining (Movie 1; cf. Fig. 1*e*). Although associations between PBs and SGs were frequently observed, these two dynamic structures remained separate entities throughout the experiment as previously reported (21). Further, the relative amounts of EGFP-Ago2 at PBs remained unchanged throughout the time course (Fig. 7*b*), again suggesting that EGFP-Ago2 accumulated at SGs are additionally redistributed from the diffuse cytoplasm.

Differential Kinetic Behaviors of Ago2 at SGs and PBs. To determine whether the Argonaute protein at SGs are redistributed directly from the cytoplasm or indirectly through PBs, we examined the kinetic behavior of EGFP-Ago2 at PBs and SGs by using photobleaching and photoactivation techniques (22). Photobleaching of EGFP-Ago2 at single PBs and SGs showed distinct recovery kinetics (Fig. 2*b*). Although Argonaute proteins in SGs continuously exchanged with the cytoplasmic pool and the fluorescence at the photobleached regions in SGs recovered to their initial levels within 6 min, those at PBs never recovered fully (Figs. 2*b* and 7*c* and data not shown). Similarly slow recovery kinetics were observed at PBs for other Argonaute members (data not shown). However, other PB components, such as Dcp1a, displayed more dynamic association with PBs and continuously exchanged with the cytoplasm (21, 23) (Fig. 7*d*). The dissociation kinetics of the PB components Ago2 and Dcp1a were dissected further. We fused photoactivatable GFP to the amino termini of these two proteins and transiently cotransfected with mRFP-Dcp1a to label PBs in live HeLa cells (Fig. 2*d* and 7*e*). Consistent with the photobleaching analyses, photoactivation of PA-Ago2 at single PBs revealed a very slow off-rate of this protein. Indeed, the majority of PA-Ago2 still remained at the photoactivated PBs at the end points of experiments (Fig. 2 *c* and *d*). In contrast, PA-Dcp1a continuously exchanged out of PBs to the cytoplasm and relocated to the neighboring PBs over the same time period (broken arrows in Figs. 2*d* and 7*e*). The relative lack of exchange and the lack of change in steady-state intensity of EGFP-Ago2 at PBs upon induction of SGs suggest that the pool of Argonaute protein at the rapidly formed SGs is not from PBs but rather originates elsewhere in the cytoplasm.

Biochemical data consistently showed that Argonaute proteins associated with polyribosomes (7–10), so we then tested whether EGFP-Ago2 in SGs could dynamically exchange with these submicroscopic pools of ribosome-associated mRNAs. If Argonaute proteins at SGs are in dynamic equilibrium with those in polyribosomes, we would expect addition of translation inhibitors, such as emetine, which irreversibly stabilize the ribosomal association with mRNAs, will shift the exchanging pool toward the polyribosomes, resulting in the eventual disassembly of preformed SGs. Indeed, addition of 10 μg/ml emetine resulted in the disassembly of the hippuristanol- or arsenite-induced, Ago2-positive SGs (Fig. 2*e* and data not shown). In contrast, EGFP-Ago2 remained localized at PBs under the same conditions (Fig. 2*e* and data not shown). Therefore, Argonaute proteins in SGs possibly originate from, and dynamically exchange with, polyribosomes in the cytoplasm.

Enrichment of Short RNAs at SGs but Not PBs. To assess whether the Argonaute proteins at SGs are associating with short RNAs in these conditions, we followed the localization of a well characterized siRNA against the endogenous *CXCR4* gene (siCXCR4), which also can function as miRNA (24). To follow its localization, siCXCR4 was labeled on the 3′ end of its antisense strand with tetramethylrhodamine (TAMRA). To minimize the fluorescence of TAMRA emitted from the double-stranded form of the siRNA, a quencher BHQ-2 was substituted for the 5′ phosphate group on the sense (passenger) strand. Thus, fluorescence of TAMRA was quenched when the two strands were associated (Fig. 8, which is published as supporting information on the PNAS web site). Further, the absence of a 5′ phosphate group on the sense strand also might enhance the selection of antisense TAMRA-labeled strand into an active RISC complex (25). The quenched TAMRA-labeled siCXCR4 exhibited similar activities as compared with an unmodified siRNA duplex when tested in the well characterized system (24), in which siCXCR4 is targeted through either imperfectly or perfectly complementary interactions to the 3′ UTR of luciferase mRNAs (Fig. 8).

HeLa cells were electroporated with quenched TAMRA-labeled siCXCR4 along with luciferase constructs with different types of CXCR4 binding sites. These cells were fixed after 56 h, a period that allows the decay of endosomally localized siRNA (18), and immunolabeled with PB and SG markers. Quantitative analysis revealed that labeled siCXCR4 was not enriched at PBs (Fig. 3*a*); however, upon induction of SGs with hippuristanol, siCXCR4 signal intensity was 1.5-fold more at SGs relative to the neighboring cytoplasm (Fig. 3*b*). The degree of enrichment at SGs did not depend on the nature of siRNA binding sites in the coexpressed luciferase constructs. However, this finding might not be informative because of the presence of both endogenous CXCR4 mRNAs with a perfectly complementary site and unknown mRNAs with an assortment of partially complementary sites. The SG enrichment was not observed when the antisense RNA strand was replaced with a TAMRA-labeled DNA/LNA hybrid oligo of the same sequence, suggesting that the localization was siRNA-specific. This hybrid oligo did accumulate into endosomal-type particles, but the number of particles decreased with time and did not colocalize with either SGs or PBs (Fig. 3 and data not shown). The absence of enrichment of siRNA at PBs contradicts recent finding by Jakymiw *et al.* showing the PB localization of siRNA (18). One possible explanation for this inconsistency may be the differences in sequences of specific siRNAs and/or labeling schemes. The scheme used here minimized fluorescence from the duplex and thus favored the detection of the TAMRA-labeled strand acting as the single active strand.

Localization of Ago2 to SGs, but Not to PBs, Depends on the Presence of miRNAs. The enrichment of short RNAs at SGs prompted us to ask whether miRNAs are required for the Argonaute protein localization to these structures. This question was investigated in several clonal Dicer knockout mouse ES cell lines where localization of transiently transfected EGFP-Ago2 could be determined in the absence of endogenous mature miRNAs. As expected, these *Dicer*−/− cells were deficient in the synthesis of detectable levels of mature miRNAs (Fig. 9, which is published as supporting information on the PNAS web site), yet the pathway downstream of miRNA synthesis remained functionally intact because transfection with siRNA efficiently silenced target genes (Fig. 9). Similar to what we observed in HeLa cells, EGFP-Ago2 was concentrated in PBs in mouse wild-type ES cells (Fig. 4*a*). Surprisingly, EGFP-Ago2 also concentrated to PBs in all three tested miRNA-deficient *Dicer*−/− cell lines (Fig. 4*a*), suggesting that short RNAs generated by Dicer are not required for the Argonaute protein localization to PBs. In contrast, upon hippuristanol treatment, EGFP-Ago2, although still concentrated to PBs, now no longer associated with SGs in *Dicer*−/− cells as compared with wild-type cells (Fig. 4*b Top* and *Middle*). Quantitatively, there was no enrichment of EGFP-Ago2 at SGs relative to the cytoplasm in *Dicer*−/− cells, whereas the

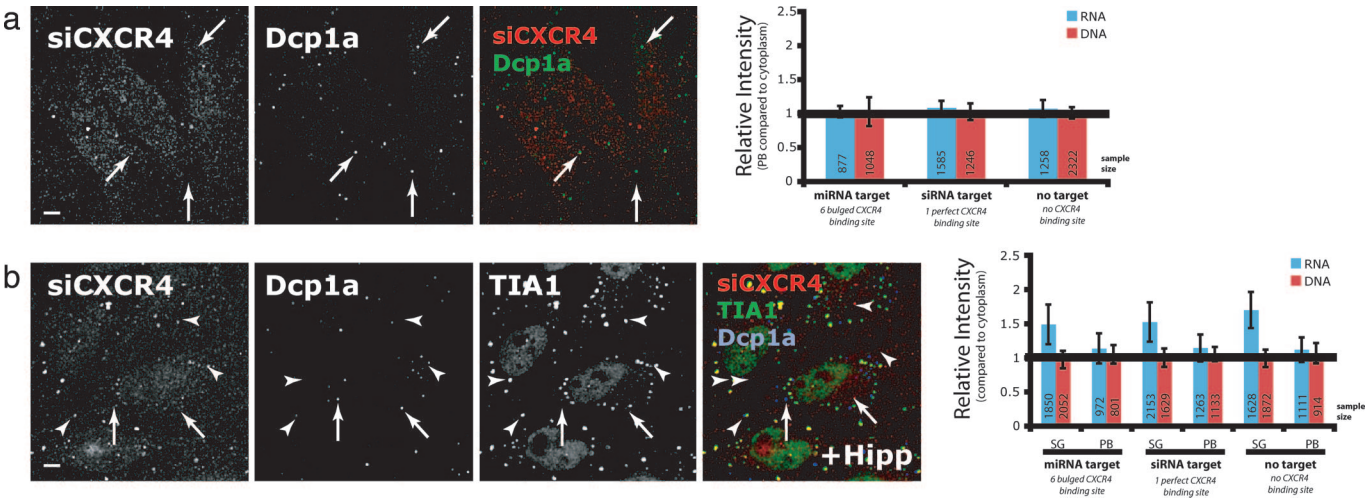

Fig. 3. Short RNAs acting as miRNAs/siRNAs enriched at SGs. (*a*) HeLa cells electroporated with 0.83 μM quenched TAMRA siCXCR4 together with different luciferase constructs containing either no binding site for siCXCR4 (no target), one perfect binding site (siRNA target), or six bulged binding sites (miRNA target) were fixed after 56 h and immunolabeled with PB marker Dcp1a. siCXCR4 did not colocalize with PBs (*Left*, arrows) and there was no enrichment of intensity observed at PBs relative to the cytoplasm (i.e., relatively intensity = 1; *Right*, blue). As a control, a similarly quenched TAMRA-labeled DNA/RNA hybrid was used to measure the degree of nonspecific nucleic acid binding (red). Note that the siCXCR4 still targets endogenous genes even though the cotransfected *Renilla* luciferase has no CXCR4 binding site (no target). (*b*) Similarly, the localization of siCXCR4 was compared with PB marker Dcp1a (arrows) and SG marker TIA1 upon addition of 1 μM hippuristanol (HIPP) for 30 min. In this case, siCXCR4 colocalized with SGs (arrowheads), but not with PBs, when translation initiation was inhibited (*Left*), as shown by the significant enrichment of the intensities at SGs compared with the cytoplasm (*Right*; two-tailed *t* test, $P \ll 0.0001$). (Scale bars, 5 μm.)

enrichment was ≈1.5-fold at SGs in wild-type ES cells (Fig. 4*c*). To test whether the absence of Argonaute protein localization to SGs depends on the presence of short RNAs generated by Dicer, we cotransfected *let7a* miRNA in the form of siRNA duplex (12) and a plasmid encoding EGFP-Ago2 into *Dicer*−/− cells. In this case, we observed that, only when exogenous miRNAs were introduced, EGFP-Ago2 was significantly enriched at SGs in miRNA-deficient *Dicer*−/− cells (Fig. 4 *b Bottom* and *c*, green). Therefore, we conclude that short RNAs are required for the Argonaute protein localization to SGs but not to PBs.

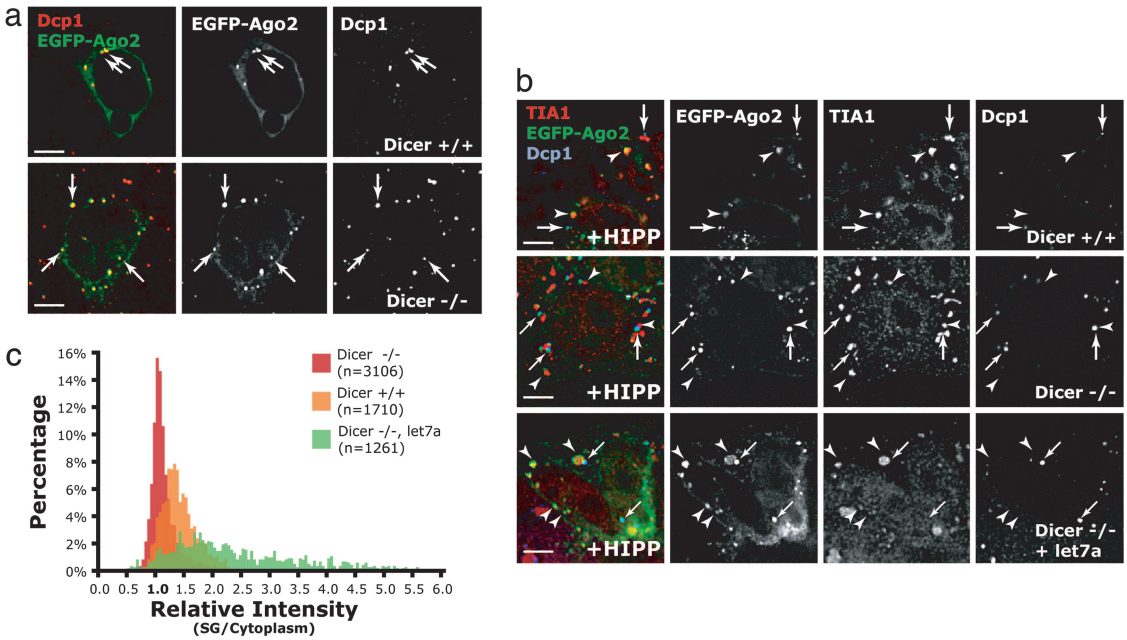

Fig. 4. The localization of Ago2 at SGs, but not at PBs, depends on the presence of short RNAs. (*a*) *Dicer*+/+ (*Upper*) and *Dicer*−/− (*Lower*) cells transiently transfected with EGFP-Ago2 were fixed after 24 h and immunolabeled with PB marker Dcp1a. In both cases, EGFP-Ago2 colocalized with PBs (arrows). (*b*) Upon addition of 1 μM hippuristanol (HIPP), transiently expressed EGFP-Ago2 still colocalized with PB marker Dcp1a in both *Dicer*+/+ (*Top*, arrows) and *Dicer*−/− (*Middle* and *Bottom*) cells. However, EGFP-Ago2 no longer colocalized with SG marker TIA1 (arrowheads) in *Dicer*−/− cells. Cotransfection of 100 nM of miRNA *let7a* in the form of siRNA duplex resulted in the localization of EGFP-Ago2 at SGs in *Dicer*−/− cells (*Bottom*). (*c*) The intensities of EGFP-Ago2 at SGs were compared with the cytoplasm in each case, and a histogram was plotted with the percentage of SGs as the *y* axis, for each relative intensity with an interval of 0.05 difference on the *x* axis. Correlated with the image data in *b*, the intensities of EGFP-Ago2 at SGs relative to the cytoplasm were centered at ≈1.0 in *Dicer*−/− cells, suggesting that there is no enrichment of EGFP-Ago2 at SGs in the absence of short RNAs. (Scale bars, 5 μm.)

Discussion

We postulate that Argonaute-associated miRNPs are constantly undergoing dynamic exchange in the cytoplasm, e.g., faster at SGs and slower at PBs, and the observed steady-state concentration of miRNPs does not necessarily imply the exclusive location of function. Apparently stable structures, such as PBs and SGs, most likely reflect the self-organization of the dynamic interactions between proteins under particular conditions (26), where submicroscopic miRNP and mRNPs complexes flux in and out of the structures continuously. It is well established that Argonaute proteins associate with multiple proteins like GW182 (18, 19) and Dcp1/2 (16) (components of PBs), HuR (15) (a component of SGs), and rck/p54 (20) (a common component of both structures). Yet, these observed colocalizations with Argonaute protein do not mean that the miRNP functions only in these defined structures. Consistent with this, siRNA- and miRNA-mediated repression remain intact in cells devoid of microscopically visible PBs and SGs (20). Thus, it is likely that both types of RNAi-related processes can occur in submicroscopic complexes in the cytoplasm.

At PBs, miRNPs are likely to be associated with the complexes related to mRNA decay and/or storage, and such close association might account for the observed ≈2-fold reduction in the abundance of the miRNA-repressed mRNAs (27). Previous immunoprecipitation data showed that the associations between Argonaute proteins and other PB components, such as Dcp1a (16), rck/p54 (20), and GW182 (19), were protein–protein interactions rather than associated through a common RNA scaffold. Consistent with these findings, we observed that the PB association of Argonaute protein did not require miRNAs. Further, it is clear from this and other studies that the PB association of Argonaute-associated miRNP seems to be rather stable as exhibited by the slow exchange of Argonaute and its associated protein GW182 (21), in contrary to the colocalized decapping complexes. In particular, we showed here that the Argonaute protein has a very slow off-rate from PBs, and it is therefore not clear how miRNA-repressed messages localized at PBs, which associate with these slowly exchanging Argonaute proteins, reenter the polyribosomes (15). Given that miRNAs repress messages at translation either after initiation or at initiation, any ribosomal subunits must be removed from the repressed messages before their entry to PBs. Therefore, the ribosome-free PBs are most likely not the sites where miRNA-mediated translational repression occurs, but it is possible that the observed stable association, through protein–protein interactions, reinforces the repressive state by keeping the message in a translation-incompetent environment. In light of these results, miRNA-mediated translation repression is likely associated with other complexes in the cytoplasm.

We have shown here that the majority of Argonaute proteins, the signature miRNA-binding component of miRNPs, are diffusively distributed in the cytoplasm. Consistent with this finding, previous quantitative studies showed that the majority (≈80%) of miRNA *let7a* and its repressed mRNAs were not localized to PBs (12), suggesting that submicroscopic miRNPs might be distributed elsewhere in the cytoplasm. Previous biochemical studies have shown that miRNPs are found to be associated with ribosomes, in particular in polyribosomes, and a substantial amount in a fraction sedimenting slower than monosomes (7–10). This fraction is, however, devoid of miRNA-repressed mRNAs and therefore does not likely represent where miRNA-mediated repression occurs (8). On the contrary, polyribosomes are consistently associated with miRNA-repressed messages, e.g., endogenous human *lin-28* and *K-ras* mRNAs that are targeted by miRNA *let7* (ref. 8 and P. A. Maroney, Y. Yu, and T. W. Nilsen, personal communication), *Caenorhabditis elegans lin-14* and *lin-28* mRNAs by *lin-4* (9, 10), or model luciferase mRNA by siCXCR4 (11). These results suggest that, at least in some cases, these miRNPs associated with ribosomes result in translation repression in the diffuse cytoplasm.

To identify which particular pool of Argonaute proteins associates with ribosomes in the diffuse cytoplasm, we perturbed the steady-state localization by subjecting cells to translational inhibitors. Upon shifting the steady-state equilibrium by limiting translation initiation, we have shown that the Argonaute protein and short RNAs are enriched at SGs. Both the kinetics and the steady-state accumulation of Argonaute-associated miRNPs at PBs remain unchanged under these conditions, suggesting that the pool at SGs did not originate from PBs. Addition of an irreversible translation inhibitor emetine, which stabilizes the association between mRNAs and ribosomes, in this new steady state results in the relocation of Argonaute protein at SGs back to the diffuse cytoplasm. This result together with the fast recovery kinetics after photobleaching at SGs suggests that those miRNPs at SGs are continually exchanging with, and most likely originally associated with, mRNAs on polyribosomes in the cytoplasm. Remarkably, targeting of the Argonaute protein to SGs only occurs in the presence of miRNAs. This requirement suggests that only miRNA-associated Argonaute proteins are localized to SGs and hence these miRNPs at SGs most likely originate from sites of miRNA-mediated repression in diffuse cytoplasm. Alternatively, SGs might preferentially recruit the miRNA-repressed messages under stress or when translation initiation is inhibited. SGs are known cytoplasmic sites concentrated with mRNPs containing AU-rich element (ARE)-binding proteins, such as HuR, TIA1, TTP, and FXR1, during stress conditions. It therefore is tempting to speculate that similar submicroscopic miRNP–mRNP associations might be related to the reported roles of miRNAs positively and negatively regulating the ARE-mediated stability of mRNAs (15, 28).

In summary, we propose that miRNPs associated with the ribosomes are repressing translation in the diffuse cytoplasm, whereas localization to specific cytoplasmic structures, such as PBs and SGs, reflects different functional states of miRNPs. We suggest that the pool localized to SGs, which is dynamically associating with ribosomes and requires miRNAs for its localization, most likely represents a subset of Argonaute proteins formerly involved in miRNA-mediated translational repression.

Materials and Methods

Chemicals, siRNAs, and DNA Constructs. ***Chemicals.*** Hippuristanol was a gift from Jerry Pelletier (McGill University, Montreal, QC, Canada).

siRNAs. siCXCR4 (antisense: 5′-uguuagcuggagugaaaactt-TAMRA-3′) was ordered from Dharmacon (Lafayette, CO). siCXCR4 (sense: 5′-BHQ2-guuuucacuccagcuaacatt-3′) was ordered from Biosearch Technologies, Inc. (Novato, CA). siCXCR4 (antisense: 5′-tGtTaGcTgGaGtGaAaAcTt-TAMRA-3′; capital letter denotes LNA) was ordered from Exiqon (Vedbaek, Denmark). Unmodified siCXCR4, siRL, and silet7 were ordered from Dharmacon; siRL targets against the *Renilla* luciferase sequence (5′-gccaagaaguuuccuaaua-3′), and silet7 is the same as published by Pillai *et al*. (12).

Plasmids. GL3, RLTK-NO, RLTK-IP, and RLTK-6X were described previously (24). mRFP-Dcp1a and EYFP-Dcp1a were gifts from Nancy Kedersha (Harvard Medical School, Boston, MA) and Bertrand Séraphin (Centre de Génétique Moléculaire, Gif-sur-Yvette, France), respectively, and the coding sequence was excised and subcloned into PAGFP-C1 (from Angus Lamond, University of Dundee, Dundee, U.K.) to make PAGFP-Dcp1a. Similarly, coding sequence of human Ago2 was obtained from Tom Tuschl (The Rockefeller University, New York, NY) and subcloned into EGFP-C1 (Clontech, Mountain View, CA) and PAGFP-C1. Sequence maps are available on request.

Cell Lines, Transfection, and Electroporation. HeLa and HeLa(E-GFP-Ago2) cell lines were generated as described previously (29) and grown with the supplement of 600 μg/ml G418 for selection. *Dicer*+/−, *Dicer*−/− (J.M.C. and P.A.S., unpublished data), and J1 ES cells were grown as described previously (30). Effectene (Qiagen, Valencia, CA) and Lipofectamine 2000 (Invitrogen, Carlsbad, CA) were used for transient transfection of plasmids/siRNAs into HeLa cells and ES cells, respectively. For electroporation, quenched TAMRA-labeled siRNAs first dissolved in solution R were added to HeLa cells and electroporated by using I-13 protocol (Amaxa, Gaithersburg, MD). Dual luciferase assays (Promega, Madison, WI) were performed as described previously (24).

Microscopy Setup. All images were taken on a Nikon IX70-based DeltaVision RT restoration microscope equipped with an Olympus 60× N.A. 1.40 Plan-Apochromat oil immersion lens, a 3D-motorized stage, appropriate filter sets (Chroma), photometrics CoolSNAP HQ CCD-camera, and a 37°C environment chamber (Solent Scientific, Segensworth, U.K.). Details of immunofluorescence and quantitation are supplied in *Supporting Text*, which is published as supporting information on the PNAS web site.

Live-Cell 4D Imaging and Photokinetics. Cells were seeded on LabTek II chambered coverglass (Nunc, Rochester, NY), and the growth medium was replaced 3 h before imaging on the next day with an optically clear CO_2-independent culture medium (041-95180M; Invitrogen) supplemented with 20% FCS. For photokinetics experiments, the microscope was set up with an additional module of two 20-W solid-state 410-nm and 488-nm lasers for photoactivation and photobleaching experiments, respectively. Imaging parameters are supplied in *Supporting Text*.

We thank Drs. Jens Lykke-Andersen (University of Colorado, Boulder, CO), Gideon Dreyfuss (University of Pennsylvania, Philadelphia, PA), Tom Hobman (University of Alberta, Edmonton, AB, Canada), Nancy Kedersha (Harvard Medical School, Boston, MA), Jerry Pelletier (McGill University, Montreal, QC, Canada), Angus Lamond (University of Dundee, Dundee, U.K.), Bertrand Séraphin (Centre de Génétique Moléculaire, Gif-sur-Yvette, France), and Tom Tuschl (The Rockefeller University, New York, NY) for kind gifts of reagents; Dr. Alice Ting for the use of a Florimeter; and Dr. Kyla Teplitz and Eliza Vasile for the setup of microscopes. We also thank Alla Grishok, Amanda Garfinkel, and Joel Neilson for critical reading of the manuscript as well as other colleagues from the Sharp laboratory for discussions. A.K.L.L. is a recipient of a Human Frontier Science Program Long-Term Fellowship. This work was supported by National Cancer Institute Program Project Grant P01 CA42063, by National Science Foundation Grant 0218506 (to P.A.S.), and partially by National Cancer Institute Cancer Center Support (core) Grant P30-CA14051.

1. Alvarez-Garcia I, Miska EA (2005) *Development (Cambridge, UK)* 132:4653–4662.
2. Bartel DP (2004) *Cell* 116:281–297.
3. Rajewsky N (2006) *Nat Genet* 38(Suppl 1):S8–S13.
4. Esquela-Kerscher A, Slack FJ (2006) *Nat Rev Cancer* 6:259–269.
5. Valencia-Sanchez MA, Liu J, Hannon GJ, Parker R (2006) *Genes Dev* 20:515–524.
6. Filipowicz W, Jaskiewicz L, Kolb FA, Pillai RS (2005) *Curr Opin Struct Biol* 15:331–341.
7. Kim J, Krichevsky A, Grad Y, Hayes GD, Kosik KS, Church GM, Ruvkun G (2004) *Proc Natl Acad Sci USA* 101:360–365.
8. Nelson PT, Hatzigeorgiou AG, Mourelatos Z (2004) *Rna* 10:387–394.
9. Olsen PH, Ambros V (1999) *Dev Biol* 216:671–680.
10. Seggerson K, Tang L, Moss EG (2002) *Dev Biol* 243:215–225.
11. Petersen CP, Bordeleau ME, Pelletier J, Sharp PA (2006) *Mol Cell* 21:533–542.
12. Pillai RS, Bhattacharyya SN, Artus CG, Zoller T, Cougot N, Basyuk E, Bertrand E, Filipowicz W (2005) *Science* 309:1573–1576.
13. Anderson P, Kedersha N (2006) *J Cell Biol* 172:803–808.
14. Brengues M, Teixeira D, Parker R (2005) *Science* 310:486–489.
15. Bhattacharyya SN, Habermacher R, Martine U, Closs EI, Filipowicz W (2006) *Cell* 125:1111–1124.
16. Liu J, Valencia-Sanchez MA, Hannon GJ, Parker R (2005) *Nat Cell Biol* 7:719–723.
17. Sen GL, Blau HM (2005) *Nat Cell Biol* 7:633–636.
18. Jakymiw A, Lian S, Eystathioy T, Li S, Satoh M, Hamel JC, Fritzler MJ, Chan EK (2005) *Nat Cell Biol* 7:1267–1274.
19. Liu J, Rivas FV, Wohlschlegel J, Yates JR, III, Parker R, Hannon GJ (2005) *Nat Cell Biol* 7:1261–1266.
20. Chu CY, Rana TM (2006) *PLoS Biol* 4:e210.
21. Kedersha N, Stoecklin G, Ayodele M, Yacono P, Lykke-Andersen J, Fitzler MJ, Scheuner D, Kaufman RJ, Golan DE, Anderson P (2005) *J Cell Biol* 169:871–884.
22. Lippincott-Schwartz J, Altan-Bonnet N, Patterson GH (2003) *Nat Cell Biol* Suppl:S7–S14.
23. Andrei MA, Ingelfinger D, Heintzmann R, Achsel T, Rivera-Pomar R, Luhrmann R (2005) *Rna* 11:717–727.
24. Doench JG, Petersen CP, Sharp PA (2003) *Genes Dev* 17:438–442.
25. Rivas FV, Tolia NH, Song JJ, Aragon JP, Liu J, Hannon GJ, Joshua-Tor L (2005) *Nat Struct Mol Biol* 12:340–349.
26. Misteli T (2001) *J Cell Biol* 155:181–185.
27. Lim LP, Lau NC, Garrett-Engele P, Grimson A, Schelter JM, Castle J, Bartel DP, Linsley PS, Johnson JM (2005) *Nature* 433:769–773.
28. Jing Q, Huang S, Guth S, Zarubin T, Motoyama A, Chen J, Di Padova F, Lin SC, Gram H, Han J (2005) *Cell* 120:623–634.
29. Leung AK, Gerlich D, Miller G, Lyon C, Lam YW, Lleres D, Daigle N, Zomerdijk J, Ellenberg J, Lamond AI (2004) *J Cell Biol* 166:787–800.
30. Li E, Bestor TH, Jaenisch R (1992) *Cell* 69:915–926.